Improvement of Quality Factor and Reduction of Spectral Bandwidth of Microcavity OLED by Bragg Mirrors

Tahereh Dirikvand, Mehdi Zadsar*, Mina Neghabi, and Jamshid Amighian

Department of Physics, Najafabad Branch, Islamic Azad University, Isfahan, Iran

***Corresponding Author Email:** mphdzadsar@gmail.com

Regular paper: Received: Jul. 22, 2022, Revised: Oct. 22, 2022, Accepted: Oct. 22, 2022,
Available Online: Oct. 22, 2022, DOI: 10.52547/ijop.16.1.79

ABSTRACT— A green microcavity organic light-emitting diode combining an Al electrode (top mirror) with a distributed Bragg reflector (bottom mirror) was designed and fabricated to improve the quality factor (more than 51) and enable high reflectance and optimal electrical properties. Experimental results indicated a remarkable increase in electroluminescence and reduction of spectral width at half maximum. Distributed Bragg reflector (DBR) films were prepared at 550°C with a surface roughness of 0.25nm (root mean square: RMS). In addition, according to SiO_2/TiO_2 refractive indices, they obtained the highest reflection compared to all organic or inorganic DBR devices. The reflectance peak at 591 nm is 94.4% for five pairs of SiO_2/TiO_2 layers indicating good agreement with theoretical simulation samples. Microcavity Organic Light-Emitting Diode (OLED) with structure: 5 pairs of SiO_2/TiO_2/ITO(120nm) /MoO_3(5nm) /MoO_3:NPB(190nm) /NPB(10nm) /Alq_3(35nm) /BCP(5nm) /LiF(0.7nm) /AL(200nm) has a quality factor of more than 51, high luminous (30%), remarkable increase in electro-luminescence (EL) and reduction of the spectral full width at half maximum of 10.93nm. This is an applied research that was obtained after detailed investigations on OLED microcavities and has a practical aspect to solving the problems of designing and manufacturing electrical and optical systems such as organic display screens. The innovative aspect of research in the technical knowledge of designing and manufacturing OLED microcavities and achieving an optimal structure using metal mirrors and Bragg reflectors to achieve coherent light output is a new and up-to-date issue that has not been done in Iran so far. As an essential step toward realizing organic lasers, the proposed approach can be used to produce new light sources.

KEYWORDS: Exciton, Organic Light Emitting Diode, Microcavity, Optical Properties.

I. INTRODUCTION

Organic Light-Emitting Diodes (OLEDs) convert electric current to light [1]. From an optical point of view, a portion of the emitted light reflects back into the structure due to exciton recombination in the active area, at interfaces, and particularly electrode contacts, and the remainder leaves the transparent part into the environment. The critical point when it comes to the internal reflection in these structures is the ratio of reflection to transmission. In other words, these devices have a low quality of light as multiple reflections into the structure contribute to exciton recombination and reduced light output. Integration into an optical resonator, such as Fabry Pérot, would correct the bipolar behavior [2]. Accordingly, in an intelligent design, the OLED was placed in a microcavity configuration between two reflectors, achieving unique optical properties in the light output compared to regular OLEDs. These properties include controlled emission direction, enhanced color distribution and purity, and optical coherency, which is particularly useful in applications such as polariton laser structures [2], optical filters [4], LEDs [5], quantum light sources [6], and active-matrix displays [7]. Accordingly, the research community has shown great interest in microcavity OLEDs and

carried out extensive studies to prepare high-quality microcavity OLED structures [8-10]. The present study discusses the different aspects of building a device based on resonance energy exchange between photons and excitons, as well as the mechanism physics. The main objectives of this study include selecting semiconductors with the right thickness for a microcavity, designing, and fabricating the device. In this configuration, an aluminum layer was use as the top mirror and a distributed Bragg reflector (DBR) as the lower electrode. The DBR is, in fact, a thin-film layout with quarter-wavelength thickness composed of dielectrics with large and small refractive indices. When light arrives at the interface of two different dielectrics, refractive index matching results in high reflectance. In this regard, a transparent indium tin oxide (ITO) (such dielectric structures are non-conductive. To use them in optoelectronic devices, they need the coating of transparent conductive layers such as indium tin oxide (ITO) is used to provide conductive contact between this structure and the optoelectronic devices. DBR/ITO structures have a higher operating value than metallic mirrors due to the combination of selective DBR wavelength reflective reflection and ITO transparent conduction properties) electrode can ensure effective electron injection without optical compromise, and its combination with a DBR layer as the bottom mirror prevents oxide accumulation on the layers and does not affect electrical properties. The optical and electrical properties, we need uniform and suitable morphology of DBR layers because the presence of porosity in DBR dielectric layers reduces the conductivity of ITO. In addition, the formation of ambiguous interfaces in the structure can significantly impair the efficiency and optical performance of DBR. We have deposited ITO with suitable morphology on this DBR to have a conductive reflective structure. In brief, the project involved building a green OLED by Physical Vapor Deposition (PVD) for reference, fabricate DBR mirrors, and construction microcavity OLEDs with 210 and 240nm thicknesses and different detection angles for the emitted spectrum. In the theoretical simulation, multi-layer films evolution software of essential Macleod has been proposed verify the model validity. Besides, the operation temperature leads to changes in the refractive index of the material for the reflection spectrum in graded DBR mirrors. It can be concluded that the size of the aperture, changes in junction temperature and the uniformity of the deposition process have very important effects on the mode pattern distribution and the number of modes and mode transition. The summary of our experimental results as well as the assistance of the DBR simulation using the Macleod's model can be concluded that the optimized microcavity OLED (210nm) has been proposed in the promising application for high efficient and low-cost optical fiber and free space data communications in the future. One of the achievements of this project is the commercialization and production of a new generation of OLED monochrome displays using nanotechnology. For the first time in the country, Electro Optic Sairan Industries Co. produced a monochrome (green) OLED screen based on BK_7 glass with nanometer ITO coating used in the collection. Laser–based distance measuring system and get a Nano scale certificate for this product from the Nano Technology Development Headquarters.

II. THEORETICAL GROUNDWORK

The device performance depends on several parameters, including the spacing between mirrors and semiconductors in the configuration. For a microcavity OLED of length L, resonant wavelengths in the microcavity are obtained from Eq. (1) [11]-[13].

$$L = {}^{m\lambda}/_{2n} \quad (1)$$

Where m is the resonant wavelength of the mode, L is the thickness of the active OLED layer, and n is the index of refraction. Moreover, standing wave conditions must be fulfilled for stable resonance inside the cavity, which requires the emission zone to stand in the middle of the cavity at resonance wavelength. Electromagnetic waves can be trapped in the microcavity as standing waves, creating several optical modes. In most cases, the same mode is

selected for the cavity. Eq. (2) shows permitted wavelengths in the cavity [14]:

$$\lambda_C = \frac{2nL_c}{m}\cos\theta_{int} \quad (2)$$

Here n is the refractive index of the intracavity layer, L_C is the mirror separation, m is an integer number, and θ_{int} is the angle formed between the propagation wave vectors (k) with the normal. The probability of photon emission in the cavity also depends on the Purcell factor [15], $F=Q\lambda^3/V$, where Q denotes the quality factor ($Q=\lambda/\Delta\lambda$), V is the cavity volume, and λ represents the wavelength. Purcell effect reduces the exciton lifetime in the microcavity, promoting spontaneous emission and efficiency, which is critical for photon guidance and reduces cavity threshold.

III. Results and Discussion

A. *Preparing the Green OLED*

For reference, a 20mm×20mm green OLED with a 3mm×4mm light emitting part comprising .The deposited materials for reference device, consist as well as special carrier blocking layers ITO anode /MoO_3[1](HIL[2] 5nm)/ MoO_3: NPB[3] (HTL[4] 190nm) /NPB (HTL 10nm) /Alq_3[5] (EML[6] 35nm) /BCP[7](EIL 5nm) /LiF(0.7nm) /Al(cathode 200nm) was fabricated. Figure 1 shows a schematic view of the device.

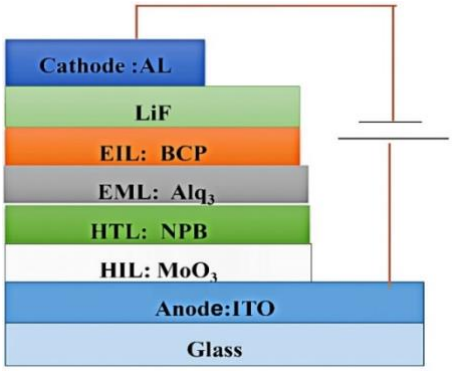

Fig. 1. Schematic view of the green OLED ITO/MoO_3 (5nm) /MoO_3: NPB (190nm) /NPB (10nm) /Alq_3 (35nm) /BCP (5nm) /LiF (0.7nm) /AL (200nm).

The procedure was as follows: The substrates were cleaned and dried with nitrogen gas. Then, an ITO film was deposited as the anode, a molybdenum trioxide (MoO_3) layer for hole injection, an NPB[8] layer for hole transport, a (BCP) hole blocking layer, and an Alq_3 emission layer. In addition, the lithium fluoride (LiF) layer was considered for electron injection and aluminum layer as a cathode. All samples were grown by PVD in a 10^{-6} mbar vacuum chamber in a passive environment to prevent damage to bottom organic layers at room temperature. The optical equipment and material thickness were simulated Macleod. A four-point probe measured the sheet resistance of the thin films. The transmitted spectrum was measured in the 300–800 nm range by a Shimadzu UV 3100 spectrophotometer before measuring the service lifetime of the OLED and its current density characteristics (J-V-L) using a Keithley 2400 source and an Ocean Optics JAZ spectrometer. The electroluminescence characteristics of the OLED were recorded at room temperature and in ambient conditions. Figure 2 plots the current–voltage characteristic and the electroluminescence spectrum of the green LED measured by the Ocean Optics JAZ spectrometer.

According to the previous works, optimization has been done and the desired structure has been used again. Therefore, due to the results obtained from spectroscopy and I-V curve, the starting voltage (the voltage at which the current flows) is about 3.2 Volts at the wavelength of 545.9 nm with the main peak and Full width at half maximum (FWHM) of 102.58 nm, with the quality factor (Q) of 6.30. This is a characteristic of an optimized green light-emitting diode. We considered this device as a reference sample and under the same conditions to compare other samples [45].

[1] Molybdenum trioxide
[2] Hole injection layers
[3] N,Nº-diphenyl-N,Nº-bis(1-naphthyl)-1,1º-biphenyl-4,4/-diamine
[4] Hole transport layers
[5] Tris (8-hydroxyquinoline) aluminum
[6] Emission layers
[7] Bathocuproine
[8] N,Nº-diphenyl-N,Nº-bis(1-naphthyl)-1,1º-biphenyl-4,4/-diamine

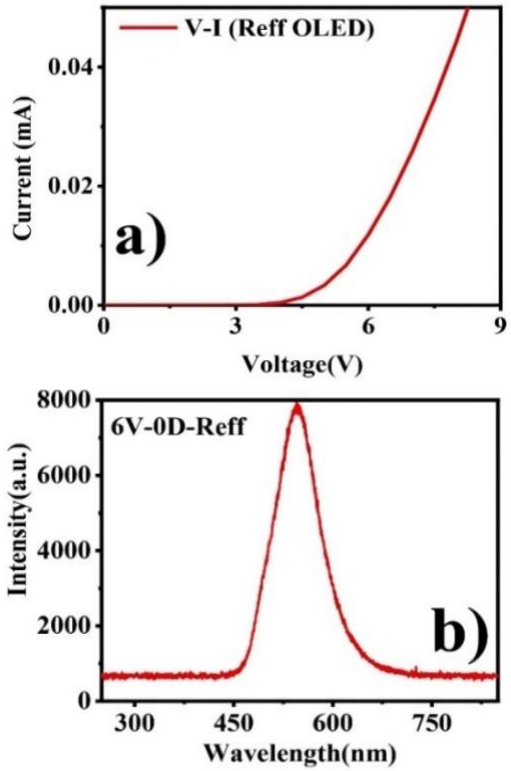

Fig. 2. a) I-V curve and b) the electroluminescence spectrum of the reference OLED.

B. *Preparing Bragg Mirrors*

Having found broad applications in electro-optical devices, DBRs have been extensively studied in recent years [16]–[20]. DBRs are commonly used in OLEDs [21], [22], LEDs [23]-[25], solar cells [26]-[27], modulators [28], [29], optical switches [30], [31], optical filters [32], [33], lasers [34], [35], and quantum light sources [36], [37]. To ensure favorable optical and electrical properties, the ITO/DBR structure requires a uniform DBR layer morphology as porosity in the layer compromises the conductivity of the ITO. Moreover, interface formation in the structure can substantially deteriorate the optical efficiency of the DBR [38]. The thin-film structure depends on deposition energy and other parameters such as substrate temperature, impurities, source energy, chemical and mechanical properties of the source material, as well as substrate topography [40]. The most important point regarding these parameters is layer growth and how atoms are stacked on the substrate [41]. In this study, nanostructured, conductive (such dielectric structures are non-conductive. To use them in optoelectronic devices, they need the coating of transparent conductive layers such as indium tin oxide (ITO) is used to provide conductive contact between this structure and the optoelectronic devices.

DBR/ITO structures have a higher operating value than metallic mirrors due to the combination of selective DBR wavelength reflection and ITO transparent conduction properties.

SiO_2/TiO_2/ITO reflectors were built by PVD. electrical resistance, crystallinity, surface roughness, and light transmission of the conductive SiO_2/TiO_2/ITO Bragg reflectors were also evaluated. Moreover, the effects of annealing on the properties were also studied. It was observe that conductive SiO_2/TiO_2/ITO Bragg reflectors had enhanced reflectance and conductivity and can be integrated as transparent conductive anodes into high-efficiency optoelectronics such as OLED microcavities. The morphological changes in DBR surface layers annealed were studied, their SEM images of which are shown in Fig. 3 (a–d) for films annealed at 250, 350, 450, and 550 °C. Raising the annealing temperature improves the surface topography of multilayer DBR films and makes a continuous structure. The surface roughness of the layers also affects the optical properties of the DBR and must be investigated [42]. Table 1. Shows the Root Mean Square (RMS) roughness of multilayer DBRs with different annealing temperatures according to analysis.

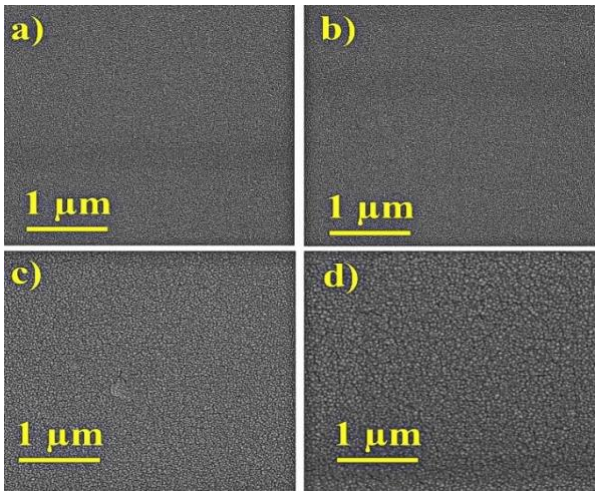

Fig. 3. The SEM images of DBR composed of 5 pairs of **S**iO_2/TiO_2/ITO thin films annealed at a) 250 °C, b) 350 °C, c) 450 °C, d) 550 °C.

Reflection specifications are critical in evaluating the optical performance of conductive DBR films. Figure 4 shows the reflection spectrum of the conductive DBR layers annealed at different temperatures in the UV and visible light range. Moreover, the reflectance of conductive DBR films increased from 85.2% at 250 °C to 94.4% at 550 °C, which can be attributed to promoted structural homogeneity and crystallinity [43].

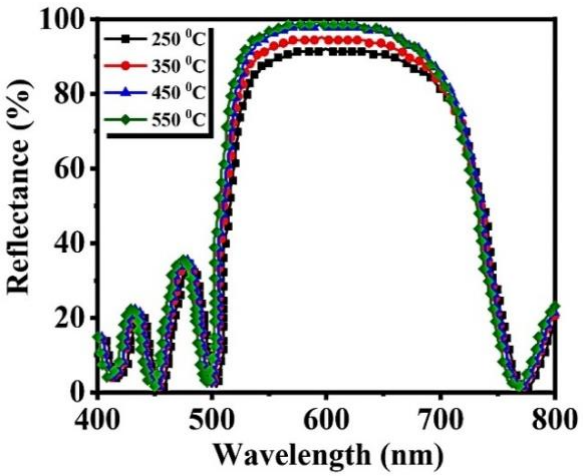

Fig .4. Optical reflectance spectra of DBR/ITO thin films at four different annealing temperatures.

Deposition with high vacuum pressure created high-purity conductive DBR thin films. Crystallinity was promoted in the 250–550°C temperature range, grain boundaries grew thinner, and charge carriers became less dispersed, increasing the carrier concentration and mobility and consequently resistance. SEM results indicate this point. Increasing annealing temperature makes the DBR layers uniform and homogeneous and reduces their surface roughness, boosting electrical current and reducing the resistance. As the annealing temperature is raised further, crystallization completes, and resistance approaches a constant level. Figure 5 depicts changes in sheet resistance.

The glass used as a substrate is BK_7 glass, which has an annealing point about of 550 ^{0}C. Therefore, the possibility of annealing at higher temperatures causes deformation of the glass structure. On the other hand, the change in the surface resistance of the sample after 450 ^{0}C is very small (10-5) and practically resistivity constant Table.1 shows the Root Mean Square (RMS) roughness of multilayer DBRs with different annealing temperatures according to analysis.

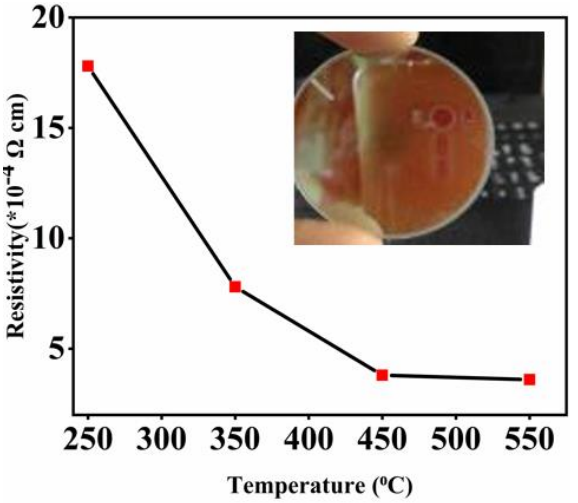

Fig. 5. Sheet resistance vs. annealing temperature (250–550 °C).

Table **1** Electrical, structural and optical properties of the different temperature annealed DBR/ITO thin films.

Annealing Temperature (°C)	RMS Roughness (nm)	Reflectance (%) at (550 nm)	Resistivity (Ω cm)
250	2.8	85.2	17.8×10^{-4}
350	2.1	89.2	7.6×10^{-4}
450	0.29	91.3	3.8×10^{-4}
550	0.25	94.4	3.9×10^{-4}

Moreover, simulation results were suggestive of the improved electromagnetic performance of the DBR mirror with five pairs of low- and high-refractive-index SiO_2 and TiO_2 layers and an ITO electrode. Figure 6 compares the simulations of three (a) and five (b) pairs of dielectric layers.

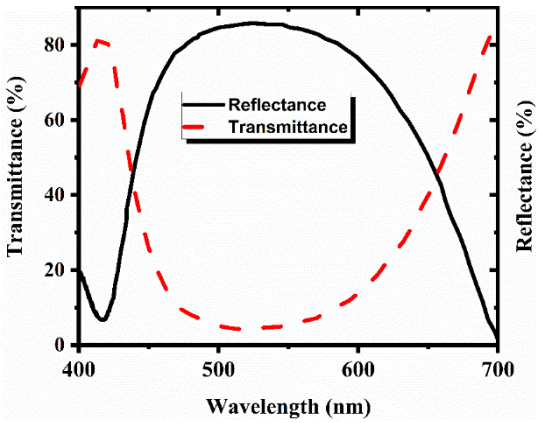

(a)

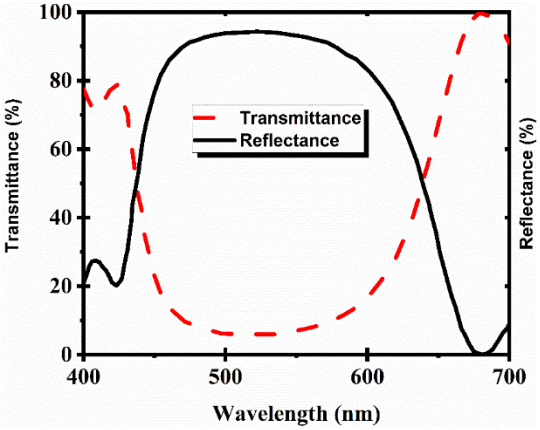

(b)

Fig. 6. Reflection–Transmission spectra (a) Three pairs of dielectrics and (b) five pairs of dielectrics.

Based on this approach, reflection, and transmission of a multilayer structure including N layers, which considered as substrate SiO_2/TiO_2 respectively [44]. The properties of a coating depend on the wavelength of light being used; the refractive indices of substrate and coating, the thickness of the coating, and the angle of the incident light samples are highly transparent for laser wavelengths and very suitable as anti-reflective front mirror. The optical matrix approach is a method, which is based on matching the electric, and magnetic field strengths of the incident light on the interface of multilayer. For n-layer antireflection coating, the matrix relation is defined as [44]; we have successfully compared the Macleod Model simulator with theoretical self-developed solution based on the Transmission Matrix (TMM), Matrix Calculating Methods (MCM) and find very good agreement with previous results.

The matrix is defined as:

$$R = \left[\frac{n_0 - Y}{n_0 + Y}\right]\left[\frac{n_0 - Y}{n_0 + Y}\right]^* \quad (3)$$

Y is optical admittance and n_0 is refractive index air, and each layer defined by:

$$M_j = \begin{bmatrix} \cos\delta_j & i\sin\delta_j \\ in_j \sin\delta_j & \cos\delta_j \end{bmatrix} \quad (4)$$

where δ_J is the phase shift, n_j is refractive index. Increasing the mirror layers evidently improves the reflectance and transmission of the emission zone. Combining DBR reflectors with transparent ITO conductors, ITO/DBR structures provide higher efficiency than regular dielectric reflectors.

The procedure can be summarized as follows:

- **S**iO_2/TiO_2/ITO thin films were prepared by thermal evaporation followed by annealing at different temperatures.
- DBR films are polycrystalline, and raising the annealing temperature was found to increase the peak intensity.
- The conductive DBR films prepared at 550 °C had a highly smooth surface with an RMS roughness of 0.25.
- The peak reflectance of the **S**iO_2/TiO_2/ITO films annealed at 550 °C reached 94.4% at 591nm wavelength.
- Increased mirror layers improve reflect-ion and transmission.

Optical behavior and cavity were carried out by using the Transfer Matrix Method (TMM) [39].

C. *Building a High-Efficiency Green OLED Using Microcavity*

High purity materials (99%) were purchased from Sigma-Aldrich, Germany. The quartz bed was prepared by sputtering deposition for the DBR mirror and ITO electrode to come on top. The thickness of each layer was optimized using the Macleod simulator to create a suitable stopband. Based on the results, the lower electrode of the OLED microcavity was prepared by growing a 75-nm-thick ITO film at 400 °C on active electrical DBRs. Moreover, Bragg diffraction conditions (quarter-wave) were also satisfied. The deposition rate and thickness were measured by quartz crystal monitor in the Angstrom Engineering thermal evaporator. We optimize the scattering conditions of a quarter of a Bragg wave and the wavelength λ_0 we considered the resonance state at 555 nm (in Macleod's simulator software). According to the results, spectral reflectance of

DBR was maximized due to the different refractive indices of the oxides growing at high temperatures. It is important to note that the Purcell effect reduces exciton lifetime in a microcavity, improving the spontaneous emission rate and internal quantum efficiency. It also plays a critical role in guiding photons to the cavity's resonance modes. All of these effects contribute to a lower lasing threshold. Considering the dependence of the Purcell effect on the quality factor, we calculated this parameter in all procedure steps. Figure.7 depicts the current–voltage characteristic and the color of the light emitted from the 240-mm-thick microcavity with a DBR/ITO lower mirror, the organic materials topping it, and an Al/LiF top mirror layer.

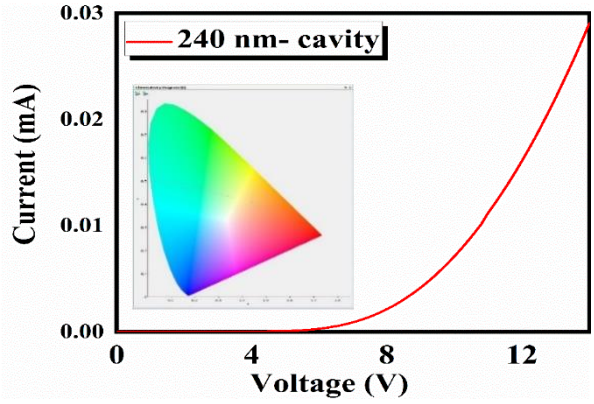

(a)

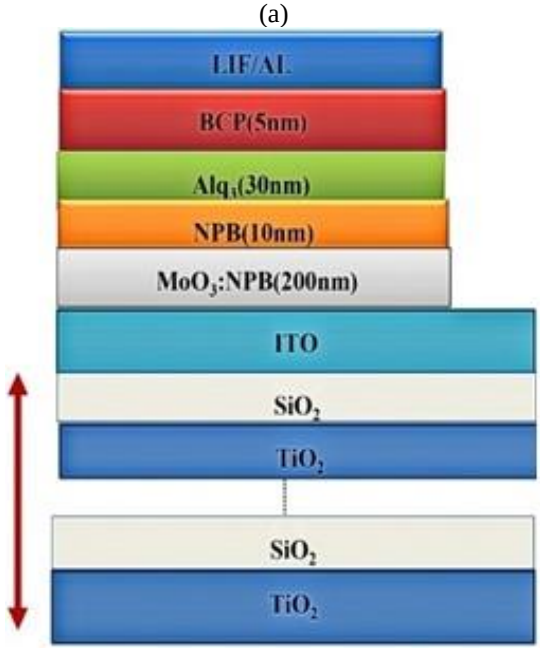

(b)

Fig. 7. a) Current density–voltage characteristic and the emission color of the 240 nm microcavity b) Schematic structure of the OLED in a DBR/Al-cathode micricavity.

Figure 8 and Table 2. Show the electroluminescence intensity against wavelength at different detection angles (0, 30 and 60° plotted as examples).

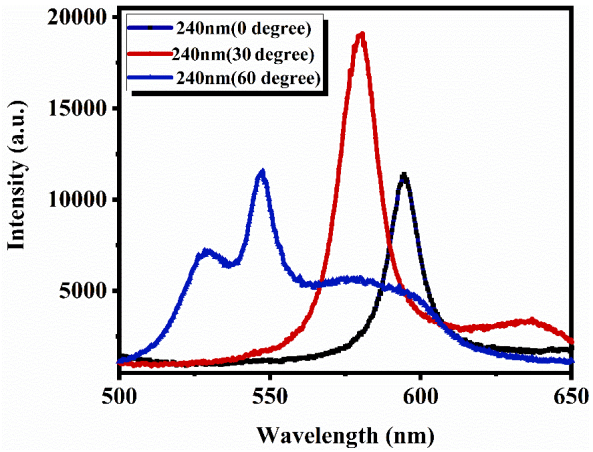

Fig. 8. Electroluminescence spectra of the microcavity OLED with angles of 0, 30 and 60 degrees(on device) detection.

Table 2. Q-factor of emission spectrum of the microcavity organic light-emitting diode 240 nm for 0 to 60 degrees detection) on device)

(°)	Peak (nm)	Intensity (L)	(FWHM) (nm)	Δλ (nm)	Factor (Q)
0	594.5	11097.5	5548.7	14.2	42.5
30	580.6	19107.9	9553.9	20.1	29.0
60	547.6	11581.6	5790.8	33.2	16.5

The data in the table are suggestive of strong orientation at 0°. Changing the detection angle increased the bandwidth while reducing the quality factor. It is evident from the table that the spectral peak remains at a specific level for different angles, which is highly useful in telecommunications and applications as an excitation source in the spectral and angular responses of the light, as well as eliminating the optical filter in a laboratory setting. As the spectrum approached the red-light range (approximately 600 nm), and according to equations 1 and 2, the microcavity thickness (p-type) was reduced from 240 to 210 nm to shift the peak toward the green light. The spectral detection was carried out at different angles and voltages with a 3cm distance from the specimen .the results are summarized in Fig. 9 and Table 3.

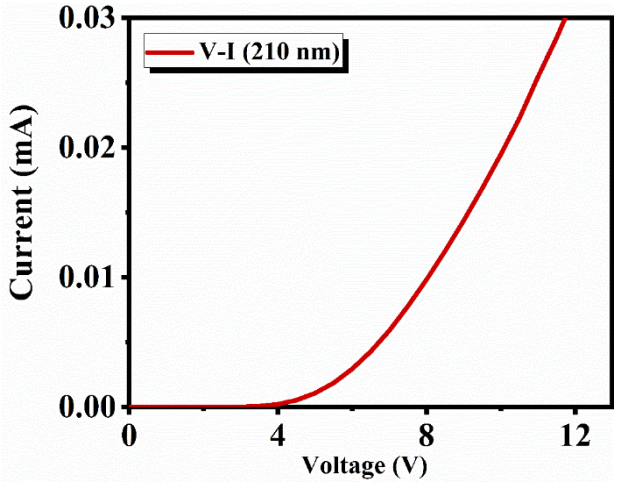

(a)

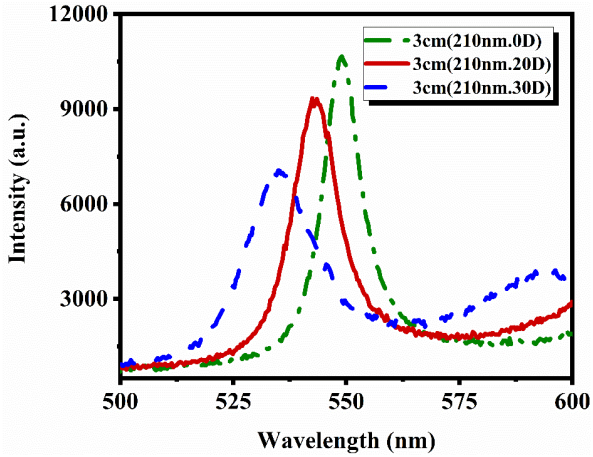

(b)

Fig. 9. a) Current density-voltage curves of a 210 nm microcavity and b) EL spectra detection at different angles of 0, 20 and 30 degrees with a 3 cm distance from the device.

Table **3.** Q-factor of emission spectra of the microcavity OLED (210nm, 3cm) for 0 to 30 degrees

Temp. (°)	Peak (nm)	Intensity (L)	FWHM (nm)	Δλ (nm)	Q-factor
0	548.9	10661.4	5330.7	10.9	50.3
10	546.5	11175.2	5587.6	12.0	45.5
20	542.4	9343.8	4671.9	14.0	38.5
30	534.9	7058.1	3529.0	22.0	24.0

As shown in the EL spectrum diagram at zero degrees of detection at a distance of 3 cm from the device, the spectrum's peak is about 550 nm with a narrower line width than other angles. This also indicates a higher quality factor. The data and diagrams of the spectrum from the 210 nm thick Micro-cavity in organic light-emitting diode (OLED) in contact with the detector at a zero-degree angle at voltages of 5, 6, and 7 volts are also shown in Fig. 10 and Table 4.

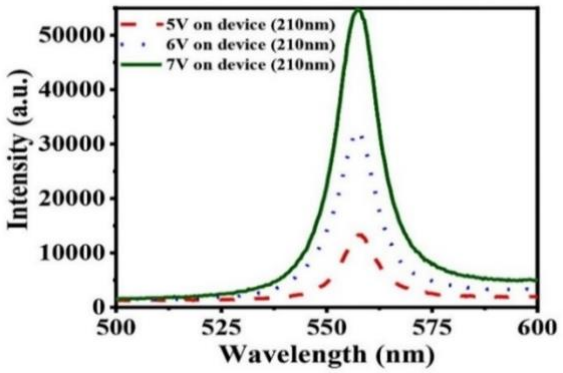

Fig.10. EL Spectra detection at different voltages and in contact with the specimen.

Table **4.** Microcavity OLED quality factor at 210 nm) on device) for different voltages

V	Peak (nm)	Intensity (L)	(FWHM) (nm)	Δλ (nm)	Q factor
7	557.2	54823.3	27411.6	13	42.8
6	557.8	32477.0	16238.5	12	46
5	557.5	13326.2	6663.1	10.9	51.01

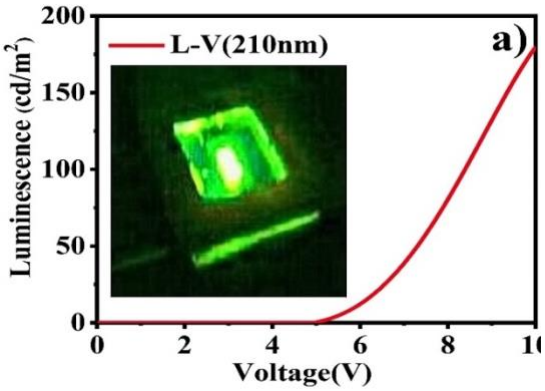

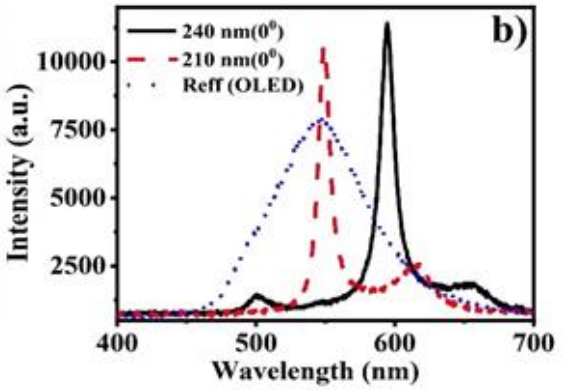

Fig. 11. a) Luminous- voltage and b) Comparison of quality factor of all three device. A: reference OLED, B: microcavity OLED with a thickness of 240 nm and: microcavity OLED with a thickness of 210 nm with a high peak at a wavelength of 555 nm

The table shows that the quality factor was obtained in three conditions of 5, 6, and 7 volts, which became the best at 5 volts. Finally, for a

more general comparison of the electroluminescence spectra diagrams, the diagrams and data of three samples: A: reference device (organic light-emitting diode without microcavity), B: microcavity OLED with a thickness of 240 nm, and C: microcavity OLED with a thickness of 210 nm made, it has been shown in Fig. 11 and Table 5. (Since the microcavity OLED is the green light, the assumed wavelength was set to 555 nanometers during the simulation with Macleod software. Then in the manufacturing process, according to the operational process and environmental conditions, the desired wavelength was measured and reported with these numbers. By changing the distance between the layers, the microcavity created the shifts, finally reaching the desired result at 557.5 nm, shown in Fig. 11.)

Comparing the obtained spectra as shown in the diagrams in Fig. 11, the spectrum contains a clear peak with a full width at half maximum (FWHM) of 10nm at the central resonance wavelength of 557.5 nm (indicating that the line width is narrower than reference device (FWHM=102.58nm). In addition, the microcavity OLED has two additional peaks at 630 and 680 nm, which can be explained by the additional bandwidth of the mirrors, which are smaller than the electroluminescence. The microcavity OLED with a thickness of 210 nm in the green light range has the best spectrum. In comparison, the microwave sample with a thickness of 240 nm has a peak at 594.5 nm, i.e., near the red light with a quality factor of 42.50, and the OLED structure without main microcavity at 545.9 nm, with a quality factor of 6.30, these results show that we made an excellent choice to increase the performance of OLEDs.

Table **5** Results corresponding to Specimens A, B, and C.

Device	Peak (nm)	FWHM (nm)	Linewidth (nm)	F.Q .
A: OLED	545/9	72952/4	102/5	6/3
B: 240nm	594/5	8455/7	14/2	42/5
C:210nm	557/5	6663/1	10/9	51/01

The emission spectra of the WMOLEDs are narrower than those of the reference OLED.

IV. CONCLUSION

A microcavity OLED was designed to improve electroluminescence and efficiency. The effects of cavity thickness were studied, showing the best results for the 210 nm microcavity. The results suggested that the microcavity OLED structure reduced the emission spectral width (10.93) and enhanced the quality factor nine-fold (51.01) compared to the reference specimen without a microcavity (A), which is a remarkable step toward optimal electroluminescence spectrum and efficiency. One application of this design is in OLED displays produced by Iran Electronics Industries, which have no domestic equivalent in the country and cannot be procured easily from international suppliers.

REFERENCES

[1] A. Genco, G. Giordano, S. Carallo, G. Accorsi, Y. Duan, S. Gambino, and M. Mazzeo "High quality factor microcavity OLED employing metal-free electrically active Bragg mirrors," Org. Electron., Vol. 62: pp. 174-180, 2018.

[2] J.H. Im, K.-T. Kang, J. S. Choi and K.H. Cho "Strong microcavity effects in hybrid quantum dot/blue organic light emitting diodes using Ag based electrode," J. Luminiscence, Vol. 203, pp. 540-545, 2018.

[3] S. Kéna-Cohen and S.R. Forrest, "Room-temperature polariton lasing in an organic single-crystal microcavity," Nat. Photon. Vol. 4, pp. 371–375, 2010.

[4] G. Hernández, *Fabry-Perot interferometers*, Cambridge University Press, 1988.

[5] H. De Neve, J. Blondelle, P. Van Daele, P. Demeester, R. Baets, and G. Borghs, "Recycling of guided mode light emission in planar microcavity light emitting diodes," Appl. Phys. Lett., Vol. 70: pp.799–801, 1997

[6] P. Lodahl, S. Mahmoodian, and S. Stobbe, "Interfacing single photons and single quantum dots with photonic nanostructures," Rev. Mod. Phys. Vol. 87: pp. 347-400, 2015.

[7] B. Geffroy, P. Le Roy, C. Prat, "Organic light-emitting diode (OLED) technology: materials, devices and display technologies," Polym. Int. Vol.55: pp. 572–582, 2006

[8] H. Sasabe and J. Kido, "Development of high-performance OLEDs for general lighting," J. Mater. Chem. C, Vol. 1, pp. 1699-1707, 2013.

[9] N.T. Kalyani and S. Dhoble, "Organic light emitting diodes: Energy saving lighting technology—a review" Renew. Sustain. Energy Rev., Vol. 16, pp. 2696-2723, 2012.

[10] R. Slusher and C. Weisbuch, "Optical microcavities in condensed matter systems. Solid state communications," Solid State Commun,Vol. 92, pp. 149-158, 1994.

[11] W. Koechner, *Solid-State Laser Engineering*, 6th Ed. Springer 2006.

[12] N. Hodgson and H. Weber *Optical Resonators*, Springer 1997.

[13] B. Masenelli, A. Gagnaire, L. Berthelot, J. Tardy, and J. Joseph, "Controlled spontaneous emission of a tri(8hydroxyquinoline) aluminum layer in a microcavity," Journal of Applied Physics, vol. 85(6), pp. 3032–3037, 1999.

[14] A.H.W. Choi, *Handbook of Optical Microcavities*, Taylor and Francis Group, 2015.

[15] E.M. Purcell, "Spontaneous emission probabilities at radio frequencies," Phys. Rev. D, Vol. 69, p. 681,1946.

[16] T. Zhi, T. Tao, B. Liu, Y. Yu, Z. Xie, H. Zhao, and D. Chen, "High Performance Wide Angle DBR Design for Optoelectronic Devices," IEEE Photon. J., Vol. 13, pp. 8200206 (1-6), 2021.

[17] R.S. Dubey and V. Ganesan, "Fabrication and characterization of SiO2/TiO2 based Bragg reflectors for light trapping applications," Results Phys., Vol. 7: pp. 2271-2276, 2017.

[18] W. Bin, H. Yingkuan, W.Yanhao, Z. Haonan, S. Bowen, Y. Xiaokun, H. Lin, W. Mingming, L Zhiyong, X Hongdi, and Z Yu "Tunable nanostructured distributed Bragg reflectors for IIInitride optoelectronic applications," RSC Adv., Vol. 10, pp. 23341-23349, 2020.

[19] L. Tao, L. Dongyu, Z. Yuan, Y. Meng, W. Yuan, Y. Taoxiang, S. Meiling, H. Yongqing, S. Youming, C. Yiming, and F. Wenjing "Design of monolithic distributed Bragg reflector-integrated photodiode using a tapered waveguide with INP and polymer cladding layer," Opt. Laser Technol., Vol. 144, pp. 107395 (1-6), 2021.

[20] R.P. Sarzala, P. Spiewak, W. Nakwaski, and M. Wasiak, "Cavity designs for nitride VCSELs with dielectric DBRs operating efficiently at different temperatures," Opt. Laser Technol, Vol. 132, pp. 106482 (1-8), 2020.

[21] T. Kitabayashi, T.A, N.Satoh, T. Kiba, M. Kawamura, Y. Abe, and K.H. Kim, "Fabrication and characterization of microcavity organic light-emitting diode with CaF2/ZnS distributed Bragg reflector," Thin Solid Films, Vol. 699, pp. 137912 (1-6), 2020.

[22] J. Lin, Y. Hu, and X. Liu, "Microcavity-Enhanced Blue Organic Light-Emitting Diode for High-Quality Monochromatic Light Source with Nonquarterwave Structural Design", Adv. Opt. Mater., Vol. 8, pp. 1901421 (1-11), 2020.

[23] A.A. Sharhan, "Transfer Matrix Mathematical Method for Evaluation the DBR Mirror for Light Emitting Diode and Laser," In J. Phys., Conference Series, IOP Publishing 2020.

[24] S.Y. Lee, J.H. Moon, Y.-T. Moon, C.S. Kim, S. Park, J.-T. Oh, H.-H. Jeong, T.-Y. Seong, and H. Amano "Improved light output of AlGaInP-based micro-light emitting diode using distributed Bragg reflector," IEEE Photon. Technol. Lett. Vol. 32, pp. 438-441, 2020.

[25] S. Zhou, C. Zheng., J. Lv, Y. Gao, R. Wang, and S. Liu, "GaN-based flip-chip LEDs with highly reflective ITO/DBR ptype and via hole-based n-type contacts for enhanced current spreading and light extraction," Opt. Laser Technol., Vol. 92, pp. 95-100, 2017.

[26] X. Chen, W. Kong, T. Chen, H. Liu, G. Huang, and R. Shu, "High-repetition-rate, sub-nanosecond and narrow-bandwidth

fiber-laser-pumped green laser for photon-counting shallow-water bathymetric Lidar," Results Phys., Vol. 19, pp. 103563 (1-7), 2020.

[27] J. Wang, Y. Xuan, Y. Da, Y. Xu, and L. Zheng, "Benefits of photonic management strategy for highly efficient bifacial solar cells," Opt. Commun.,: Vol. 462, pp. 125358 (1-8), 2020.

[28] H. Liu, S. Zhang, H. Ding, W. Sun, and L. Sun, "Investigation on the optical dual-band absorption enhancement for graphene photodetector," Results Phys.,Vol. 29, pp. 104747 (1-6), 2021.

[29] M. Xu, M. He., X. Liu, Y. Pan, S. Yu, and X. Ca, "Integrated lithium niobate modulator and frequency comb generator based on Fabry-Perot resonators," In CLEO: A and T. Optical Society of America. 2020.

[30] D. Admassu, T. Durowade, R. Sellers, and S. Sivananthan, "Effect of interface grading on the optical performance of distributed Bragg reflector multilayers in Fabry-Pérot optical filters," Micro. Technol., Vol. 27, pp. 2785-2790, 2021.

[31] Y. Wu, X. Zhao., J. Hu, and H. Xu,"Low threshold optical bistability based on coupled graphene Tamm states," Results Phys., Vol. 21: pp. 103824 (1-5), 2021.

[32] I. A. Derebezov, V.A. Haisler, A V Haisler, D. V. Dmitriev, A. I. Toropov, S. Rodt, M. von Helversen, C. de la Haye, S. Bounouar and S. Reitzenstein," Quantum light sources based on deterministic microlenses structures with (111) In (Ga) As and AlInAs QDs". J. Phys.: Conf. Ser. Vol. 1461, pp. 012028 (1-7). IOP Publishing, 2020.

[33] D. Zhou, S. Liang, Y. He, Y. Liu, D. Lu, L. Zhao and W. Wang, "Two 10 Gb/s directly modulated DBR lasers covering 20 nm wavelength range", Opt. Commun., Vol. 475, pp. 126236 (1-4), 2020.

[34] Y. Tao, S. Zhang., M. Jiang, C. Li, P. Zhou, and Z. Jiang,, "High power and high efficiency single-frequency 1030 nm DFB fiber laser," Opt. Laser Technol., Vol. 145, pp. 107519 (1-5), 2022.

[35] X. Wang, L. Wang, J. Wang, and F. Wang, "High sensitivity interrogation system of fiber Bragg grating sensor with composite cavity fiber laser," Opt. Laser Technol., Vol. 142, pp. 107228 (1-6), 2021.

[36] W. Li, Y.X. Qi, S.P. Liu, and X.Y. Maa, "High power density and temperature stable vertical-cavity surface-emitting laser with a ring close packing structure," Opt. Laser Technol., Vol. 132, pp. 106510 (1-8), 2020.

[37] Y. Trabelsi, N. Ben Ali, F.S. Chaves,,and H.V. Posada, "Photonic band gap properties of one-dimensional photonic quasicrystals containing Nematic liquid crystals," Results Phys., Vol. 19, pp. 103600 (1-8), 2020.

[38] T. Akagi, Y. Kozuka, K. Ikeyama, S. Iwayama, M. Kuramoto, T. Saito, T. Tanaka, T. Takeuchi, S. Kamiyama, M. Iwaya. and I. Akasaki, "High-quality AlInN/GaN distributed Bragg reflectors grown by metalorganic vapor phase epitaxy." Appl. Phys. Express, Vol. 13, pp. 125504 (1-4), 2020.

[39] P. Yeh, *Optical waves in layered media*, Wiley Interscience, 2005

[40] C. Wang, W.D. Li., Z.H. Jiang, X. Yang, G.Y. Sun, and G.J. Zhang "UV-cured nanocomposite coating for surface charging mitigation and breakdown strength enhancement: exploring the combination of surface topographical structure and perfluorooctyl chain," R. Soc. Chem. Adv., Vol. 10, pp. 16422-16430, 2020.

[41] L. Yafei, H. Peng, Z .Chen, T. Ailihuamaer, S. Hu, B. Raghothamachar, and M. Dudley "Application of synchrotron X-ray topography to characterization of ion implanted GaN epitaxial layers for the development of vertical power devices," Mater. Res. Adv., Vol. 6, pp. 450-455, 2021.

[42] S. Gandrothula, T. Kamikawa., J.S. Speck, S. Nakamura, and S.P. DenBaars, "Study of surface roughness of lifted-off epitaxial lateral overgrown GaN layers for the n-DBR mirror of an III-nitride vertical-cavity surface emitting laser," Appl. Phys. Express, Vol. 14, pp. 031002 (1-8), 2021.

[43] P. Giusto, P. Lova, G. Manfredi, S. Gazzo, P. Srinivasan, S. Radice, and D. Comoretto, "Colorimetric detection of

perfluorinated compounds by allpolymer photonic transducers," ACS Omega, Vol. 3, pp. 7517-7522, 2018.

[44] O. Duyar and H.Z. Durusoy,"Design and preparation of antireflection and reflection optical coatings," Turk. J. Phys., Vol. 28, pp. 139–144, 2004.

[45] M. Zadsar, H.R. Fallah, M.H. Mahmoodzadeh, and S.V. Tabatabaei, "The effect of Ag layer thickness on the properties of WO_3/Ag/MoO_3 multilayer films as anode in organic light emitting diodes," J. Luminescence, Vol. 132, pp. 992-997, 2012.

Tahereh Dirikvand was born in Isfahan , Iran on 21 September 1980. She received the BSc degree in 2003 and the MSc degree in Atomic Molecular Physics in 2015 from University of Isfahan, Isfahan, Iran. In 2016, She started studying for a PhD degree in Physics at University of Najafabad, Iran. She is currently working as a lecturer in the Islamic Azad University of Najafabad while conducting research in the field of physics.

Jamshid Amighian was born in Isfahan on 22 march 1945. He recieved his BSc in physics from Isfahan University in 1967 and his PhD on solid state physics from Durham University, England in 1975. He has been an academic member at Physics Department of Isfahan University and after retirement, as a full professor, he joint the Islamic Azad University of Najafabad. He has published many papers and translated a few books sush as Introduction to solid state physics by C. Kittel, Elements of X ray Diffraction by B.D. Cullity, Modern Physics and Quantum mechanics by E.E. Anderson. He has also supervised many MSc and PhD theses.

Mina Neghabi was born in Isfahan, Iran, on September 5, 1982. She received the BSc degree in Physics in 2004 from University of Kashan, Kashan, Iran and the MSc degree in Atomic, Molecular Physics in 2006 from University of Yazd, Yazd, Iran. In 2011, she obtained the PhD degree in Atomic, Molecular Physics from University of Yazd.

Now, she is an assistant professor at Islamic Azad University, Najafabad Branch from 2008

Mehdi Zadsar was born in Kashan, Iran, on January 10, 1981. He received the BSc degree in Physics in 2004 from University of Kashan, Kashan, Iran and received the MSc degree in Atomic, Molecular Physics in 2007 from University of Isfahan, Isfahan, Iran. In 2012, he obtained the Ph.D. degree in Atomic, Molecular Physics from University of Isfahan.

He is assistant professor at Islamic Azad University, Najafabad Branch from 2008.